RadioGraphics

Can CT Pulmonary Angiography Allow Assessment of Severity and Prognosis in Patients Presenting with Pulmonary Embolism? What the Radiologist Needs to Know[1]

Benoît Ghaye, MD • Alexandre Ghuysen, MD • Pierre-Julien Bruyere, MD
Vincent D'Orio, MD, PhD • Robert F. Dondelinger, MD

SUPPLEMENTAL MATERIAL

Movie clips to supplement this article are available online at radiographics.rsnajnls.org/cgi/content/full/26/1/23/DC1.

TEACHING POINTS

See last page

Computed tomographic (CT) pulmonary angiography has been established as a first-line diagnostic technique in patients suspected of having pulmonary embolism. Risk stratification is important in patients with pulmonary embolism because optimal management, monitoring, and therapeutic strategies depend on the prognosis. Acute right-sided heart failure is known to be responsible for circulatory collapse and death in patients with severe pulmonary embolism. Acute right-sided heart failure can be assessed at CT pulmonary angiography by measuring the dimensions of right-sided heart cavities or upstream venous structures, such as the superior vena cava or azygos vein. The magnitude of pulmonary embolism can be calculated at CT pulmonary angiography by applying angiographic scores adapted for CT (Miller and Walsh scores) or dedicated CT scores (Qanadli and Mastora scores). The advent of CT pulmonary angiography performed with electrocardiographic gating permits new advances in assessment of acute right-sided heart failure, such as measurement of the ventricular ejection fraction. Although such findings may be useful for assessment of treatment effectiveness, their effect on prognosis in patients with severe pulmonary embolism is debated in the literature.

Abbreviations: DVT = deep venous thrombosis, ECG = electrocardiography, IVC = inferior vena cava, LV = left ventricle, PA = pulmonary artery, PE = pulmonary embolism, RV = right ventricle

RadioGraphics 2006; 26:23–40 • **Published online** 10.1148/rg.261055062 • **Content Codes:** CH CT

[1]From the Departments of Medical Imaging (B.G., P.J.B., R.F.D.) and Medicine (A.G., V.D.), University Hospital of Liege, Sart Tilman B35, B-4000 Liege, Belgium. Recipient of a Certificate of Merit award for an education exhibit at the 2004 RSNA Annual Meeting. Received March 24, 2005; revision requested April 28 and received July 11; accepted August 18. All authors have no financial relationships to disclose. **Address correspondence to** B.G. (e-mail: *bghaye@chu.ulg.ac.be*).

See the commentary by Balachandran et al following this article.

Introduction

Despite advances in prophylaxis, diagnostic modalities, and therapeutic options, venous thromboembolism remains a major health problem, with an incidence of around 1.5 per 1,000 person-years (1). In two recent large multicentric studies, although a high mortality rate of 50%–58% was found in patients presenting with hemodynamic instability, a 8%–15% mortality rate was still reported in hemodynamically stable patients (2,3). As death frequently occurs within the first hours after admission, a rapid and specific diagnosis is required (4). When severe, pulmonary embolism (PE) can induce acute right heart failure, eventually resulting in circulatory collapse and death. As a correlation between right ventricular (RV) dysfunction detected at echocardiography and clinical outcome has been shown (2,5–10), echocardiography has been advocated as a first-line test in hemodynamically unstable patients in order to promptly start a fibrinolytic therapy (3,5,11).

Computed tomographic (CT) pulmonary angiography has progressively been established as the frontline imaging modality for the diagnosis of PE, replacing ventilation-perfusion lung scintigraphy and pulmonary angiography (12–14). CT pulmonary angiography has also become more frequently included in recommended diagnostic algorithms (15,16). Compared to echocardiography, CT pulmonary angiography has the advantage of allowing a more comprehensive assessment of the clot burden in the pulmonary arteries (PAs), associated underlying lung disease, and other causes of acute chest pain (12,17,18). Therefore, it is essential that radiologists know how to evaluate the severity of the current episode of PE at CT pulmonary angiography.

The purpose of this article is to review use of CT findings for predicting the severity of PE. The findings are divided into those that are not controversial, those that are controversial, and finally findings that are still experimental or under evaluation.

Pathophysiology of Fatal Outcome in Severe PE

Under physiologic conditions, the interaction between the RV and the relatively low pulmonary vascular impedance results in a pressure less than one quarter that of the left ventricle (LV). The RV operates at rest at a maximum efficiency level, and stroke work is achieved with the minimum oxygen consumption. Acute embolic obstruction of a significant amount of the pulmonary circulation (usually estimated as more than 30%) increases pulmonary vascular resistances, leading to acute PA hypertension (Fig 1). Abrupt pulmonary vascular obstruction occurring during PE is further worsened by the release of vasoactive agents from plasma, platelets, or tissue and reflex PA vasoconstriction, leading to systemic arterial hypoxemia (4,19,20).

Teaching Point

The clinical impact of the embolic event depends not only on the embolus size but also on the underlying cardiopulmonary status. Indeed, the RV may compensate for RV outflow obstruction by using the Frank-Starling mechanism and, eventually, increased contractile performance. However, this compensation requires an increase in work transmission from the RV to its vascular bed, leading to a greater myocardial oxygen demand and a reduction in RV mechanical efficiency. Besides, pericardial constraint and RV dilatation cause bowing of the interventricular septum toward the LV, resulting in a decreased LV preload (21,22). Subsequently, decreased LV output and decreased systemic arterial pressure may result in a downward vicious circle of compromised coronary perfusion, increasing ventricular hypoxemia and RV dysfunction, and eventually cardiogenic shock, RV infarction, and finally circulatory collapse (4,5,23).

Assessment of the Severity of PE

Clinical Identification of High-Risk Patients

Estimation of acute PE clinical outcome in the International Cooperative Pulmonary Embolism Registry (ICOPER) and Management Strategy and Prognosis of Pulmonary Embolism Registry (MAPPET) studies underlined the importance of circulatory failure and systemic hypotension as predictors of poor prognosis (2,3). Nevertheless, hemodynamically unstable PE constitutes only a minority of all PE presentations (4). Therefore, other clinical predictors of poor outcome are required. Age over 70 years, coexisting congestive heart failure, or chronic obstructive pulmonary disease have also been identified as significant prognosis factors (2), mainly because preexisting cardiopulmonary dysfunction impairs RV adaptability to abrupt afterload increase. In patients with normal systolic arterial pressure, mortality increases with worsening of RV dysfunction (3,8–10).

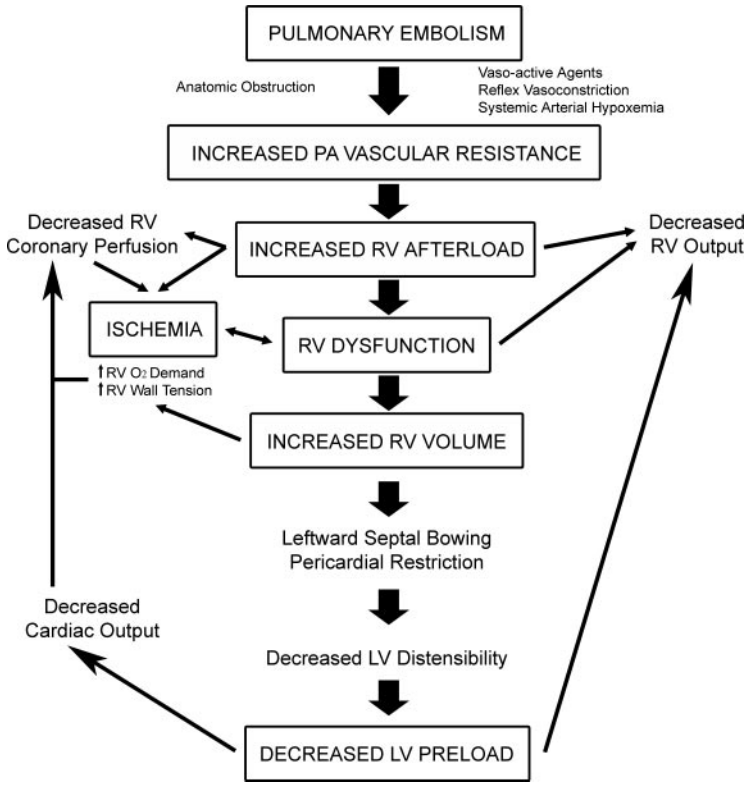

Figure 1. Pathophysiologic cycle of major PE (4,5).

Therefore, clinical examination should aim at the identification of signs of acute RV dysfunction, including tachycardia, low arterial blood pressure, distended neck veins, accentuated pulmonic second heart sound (P_2), or tricuspid regurgitation murmur. RV strain at electrocardiography (ECG) (T-wave inversion or pseudoinfarction pattern in anterior leads) is closely related to RV dysfunction and is an independent predictor of adverse clinical outcome (24). Moreover, cardiac biomarkers, including troponins and natriuretic peptides, have emerged as useful tools for risk assessment and optimizing management strategy in patients with acute PE (25).

Imaging Assessment of the Severity of PE

Echocardiography.—Echocardiography can be used as the first-line method in unstable patients as it allows the diagnosis of acute right heart failure, permits visualization of clots in the right heart cavities or in some locations of the central PA, and may provide alternative diagnoses, such as aortic dissection, pericardial disease, myocardial infarction, and valvular insufficiency (3,4).

Echocardiography can be helpful in assessing patients with PE by demonstrating RV dilatation and hypokinesis; straightening, leftward bowing, or paradoxical motion of the interventricular septum; decreased LV volume ("empty LV" appearance); loss of inspiratory collapse of the inferior vena cava (IVC); tricuspid regurgitation; and dilatation of the PA (21,26–28). The McConnell sign, a distinct echocardiographic pattern of regional RV dysfunction in which the apex is spared, appears to be specific for acute PE (29). The presence of RV hypertrophy (wall thickness $>$ 5–6 mm) helps differentiate between acute and subacute or chronic massive PE (30). In addition to demonstrating the hemodynamic effect of PE, echocardiography allows assessment of the prognosis of acute PE. The presence of an acute RV afterload dysfunction is associated with high in-hospital mortality and a high rate of complications, whereas its absence can be considered a sign of a good prognosis (3,7).

Transesophageal echocardiography performs better than transthoracic echocardiography in the diagnosis of PE (31). Transesophageal echocardiography is limited by operator dependence, topographic limitations due to air contained in the lung and central airways, and patient-related factors, which may limit the technical quality of echocardiography in up to 40% of cases (31).

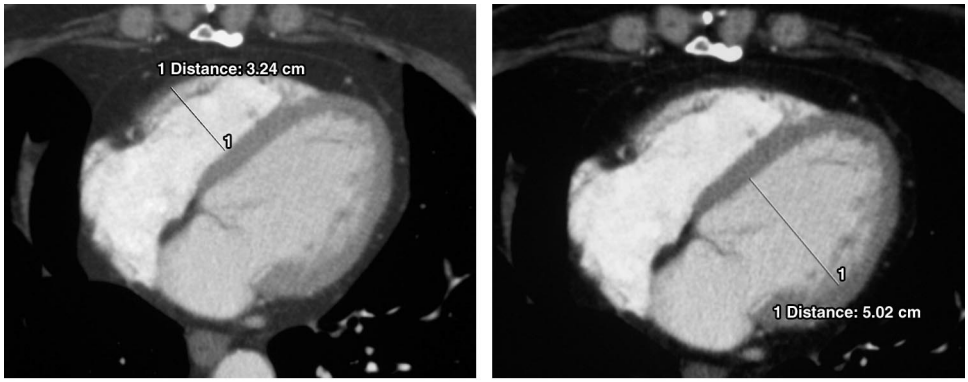

a. **b.**

Figure 2. Measurement of the short axes of the RV and LV on axial CT pulmonary angiograms. **(a)** The short axis of the RV is measured at the level of the tricuspid valve from inner wall to inner wall at the widest point, which is typically in the basal third of the ventricle. **(b)** The short axis of the LV is measured at the level of the mitral valve from inner wall to inner wall at the widest point, which also is typically in the basal third of the ventricle. Note that the short axes of the RV and LV may be located at different axial CT levels.

Echocardiography also has limitations in demonstrating PE as the cause of RV pressure overload. When no endoluminal clots are evident, other confirmatory studies for PE are therefore required in stable patients (4,6,7,11).

Computed Tomography.—Owing to limitations of echocardiography in demonstrating PE as the cause of RV pressure overload, it is desirable that a single test, namely CT pulmonary angiography, allow accurate diagnosis of venous thromboembolic disease, assessment of the severity of PE, and prediction of the patient's outcome. The severity of PE can be evaluated at CT by using different aspects, from the PE itself to upstream consequences and ultimately the origin of PE, namely venous thrombosis: *(a)* the obstruction of the pulmonary vascular bed; *(b)* the consequences of pulmonary vascular bed obstruction at the level of the heart; *(c)* upstream consequences at the level of abdominal and thoracic venous structures; and *(d)* the clot burden in lower limb and abdominal veins, which represents the risk for recurrent episodes of PE.

For practical purposes, we will present the 2005 state of the art by discussing separately findings that are not controversial, findings that are controversial, and finally findings that are still experimental or under evaluation.

Noncontroversial Findings

Previous studies have reported that RV failure, resulting from both the volume of embolus and underlying cardiopulmonary function, is a more accurate indicator of the severity of PE than the degree of obstruction at angiography or scintigraphy (32–35). Obstruction of more than 30% of the pulmonary circulation causes sufficient elevation of the pulmonary vascular resistance to produce significant pulmonary hypertension, resulting in RV afterload increase and dilatation (4,36). The cardiovascular effects of any acute PE must be regarded not only as the result of the degree of pulmonary vascular bed obstruction but also as the potential for the RV to turn into a high-pressure pump. In other words, failure occurs if thin RV walls do not succeed in compensating for the sudden elevation in parietal tension. It is the uncoupling of RV resources to the pulmonary vascular load rather than the obstruction index per se that leads to RV dilatation and dysfunction, including successively decreased stroke volume, tricuspid regurgitation, reduced venous return, and finally circulatory collapse (4).

Cardiac CT Measurements

Quantitative cardiac CT measurements obtained on axial CT images, namely the RV short axis, the LV short axis, and particularly the RV/LV short axes ratio, have shown a significant positive (RV short axis, RV/LV diameter ratio) or negative (LV short axis) correlation with the severity of PE (37) or with fatal outcome (38,39) (Fig 2). In two

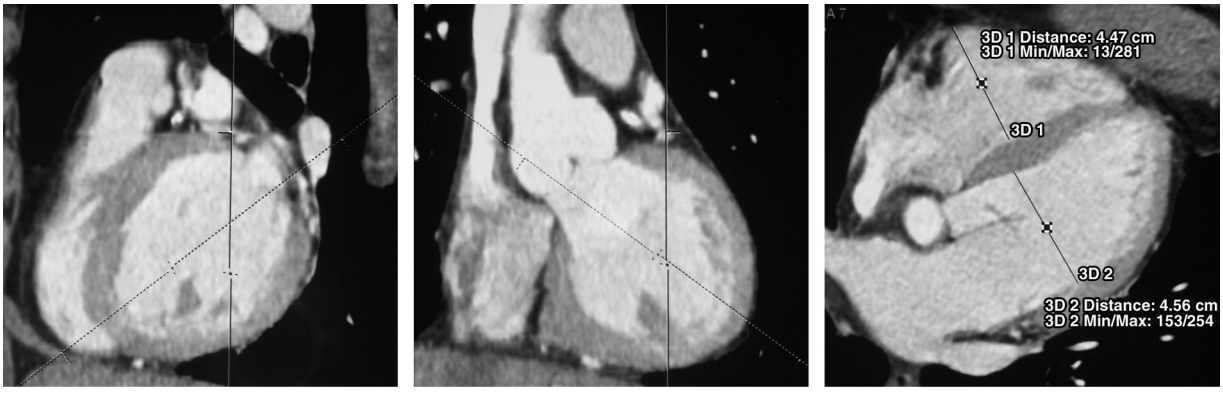

a. b. c.

Figure 3. Measurement of the short axes of the RV and LV on a reformatted four-chamber CT image obtained in a 54-year-old patient with nonsevere PE. Dashed lines on sagittal **(a)** and coronal **(b)** CT images of the heart are rotated to obtain the four-chamber image **(c)**. The short axes of the RV and LV are 44.7 mm and 45.6 mm, respectively, resulting in a normal RV/LV diameter ratio of less than 1.

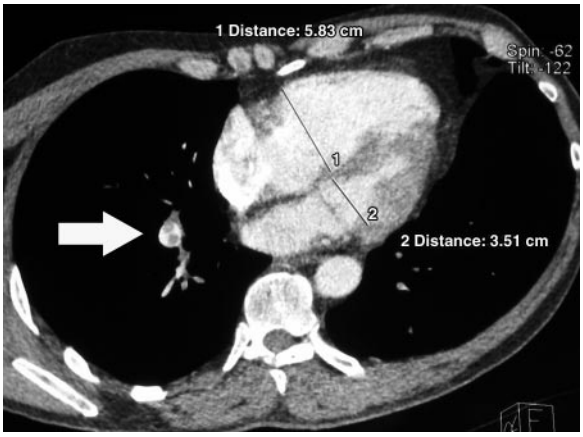

Figure 4. Moderate acute dilatation of the RV in a 55-year-old man with massive PE. Four-chamber CT image shows measurements for the short axes of the RV and LV, resulting in an RV/LV diameter ratio of 1.7. Note the PE in the right lower lobe PA (arrow).

studies of 25 patients with PE and 14 patients with massive PE, Contractor et al (23) and Lim et al (40) found that signs of RV strain at CT pulmonary angiography (RV/LV diameter ratio > 1, leftward septal bowing) had a sensitivity of 78%–92%, specificity of 100%, and positive predictive value of 100% when compared to echocardiographic findings for the detection of RV dysfunction. Additional studies have estimated that an RV/LV diameter ratio superior to 1.5 indicates a severe episode of PE (36–39,41). In the study by Araoz et al (42), an RV/LV diameter ratio greater than 1 was associated with a 3.6-fold increased risk of admission to the intensive care unit. Moreover, Ghaye et al (39) recently demonstrated a significant relation between the RV/LV diameter ratio and the risk of death in 82 patients who presented with a severe PE-related clinical condition that required admission to the intensive care unit.

Teaching Point

As CT images obtained in the axial plane are not a four-chamber view, relative measurements may be different from those of echocardiography (18,23,37). Quiroz et al (18) reported that ventricular CT measurements obtained from a four-chamber view were different from those obtained on axial views and closer to echocardiographic values (Figs 3, 4). An RV/LV diameter ratio greater than 0.9 calculated on a four-chamber view was associated with a sensitivity of 83% and specificity of 49% for predicting the occurrence of adverse clinical events (defined as 30-day mortality or the need for cardiopulmonary resuscitation, mechanical ventilation, vasopressors, thrombolysis, or embolectomy) (18). More recently, the same group of investigators reported a higher mortality rate in patients with an RV/LV diameter ratio greater than 0.9 compared to an RV/LV diameter ratio less than or equal to 0.9 calculated on a four-chamber view in 431 patients with PE. RV enlargement had a sensitivity, specificity, positive predictive value, and negative predictive value of 78.2%, 38%, 15.6%, and 92.3%, respectively, for prediction of 30-day mortality (43).

Even more precise estimation of the heart dimensions could be achieved by measuring the ratio of ventricular areas instead of the ratio of short axes (28,41).

Diameters of the Superior Vena Cava and Azygos Vein

An acute increase in volume and pressure in the right heart may be associated with upstream manifestations at the level of systemic venous structures. Collomb et al (37) found significantly different diameters of the superior vena cava in patients with severe PE and patients with nonsevere PE. Furthermore, in patients with severe PE, another study reported statistically different CT diameters of the superior vena cava and azygos vein in survivors and nonsurvivors (39). Previous work based on chest radiographs by Milne and Pistolesi (44) evaluated the relationship between the mean right atrial pressure and the diameter of the azygos vein and the width of the vascular pedicle, which is mainly affected by the dimension of the superior vena cava. Both measurements were significantly correlated with mean right atrial pressure and the circulating blood volume. These authors observed an abrupt increase in size of the azygos vein and widening of the vascular pedicle in patients presenting with acute right heart failure. In support of this finding, the size of the IVC as measured at ultrasonography (US) has been shown to reflect right heart hemodynamics (26,27).

Of these cardiac and venous measurements, the RV/LV diameter ratio is the easiest to calculate and should be included in every report of a CT pulmonary angiography examination. An increased RV/LV diameter ratio may be an important finding for the clinician. Nevertheless, prospective studies are needed to determine how such a finding could affect patient care and treatment.

Controversial Findings

PA Clot Load Scores

The presence, location, and degree of obstruction of arterial clots can be scored according to four different scoring systems as proposed by Miller et al (45), Walsh et al (46), Qanadli et al (47), and Mastora et al (48). Introduced in the 1970s, the scores proposed by Miller et al (45) and Walsh et al (46) are angiographic severity indices designed to compare the rate of resolution of PE when heparin or fibrinolytics are used. Modified Miller and Walsh scores have been adapted for CT pulmonary angiography, and there was an excellent correlation between both scores and a good interobserver agreement in one study (49). The main limitation was absence of residual PA flow assessment, as these adapted scores do not allow differentiation between partial and complete obstruction of the PAs. The more recent scores proposed by Qanadli et al (47) and Mastora et al (48) were designed to quantitatively assess the severity of acute PE at CT pulmonary angiography. Details on calculation of the scores are presented in Appendix 1. Despite their methodologic differences, all scores showed an excellent correlation with each other in different studies (Fig 5) (39,47,49).

The current literature shows some discrepancies regarding the potential for association between the severity of PA clot load scores and immediate outcome, probably due to differences in the populations studied in terms of severity of PE. Wu et al (50) recently reported that patients with a PA clot load score of more than 60% tended to succumb. These authors (50) and van der Meer et al (38) found the score proposed by Qanadli et al (47) to be a significant predictor of death in 59 and 120 patients, respectively, with positive results at CT pulmonary angiography ($P = .002$).

On the other hand, Collomb et al (37) found that the severity of PA obstruction determined with the score proposed by Qanadli et al (47) can be used as an indicator of the hemodynamic severity of PE, reflected by a mean Qanadli score of 54% ± 11 in patients with severe PE (ie, requiring thrombolytic or surgical treatment) and 24% ± 18 in patients with nonsevere PE. Similarly, Ghaye et al (39) and Araoz et al (42) reported PA clot load scores to be a poor predictor of mortality in patients with acute PE. While PA clot load scores can be an indicator of the severity of the current episode of PE or treatment effectiveness, it seems that they cannot be used as a predictor of RV failure and death of the patient (37,39,42). Araoz et al (42) found that the clot burden at CT was associated with the subsequent use of vasopressors in 173 patients with PE ($P = .05$).

Pulmonary vascular resistance is not only related to mechanical obstruction by the intravascular clot load but can be further increased by the release of vasoactive agents from plasma, platelets, or tissue; reflex PA vasoconstriction; and systemic arterial hypoxemia occurring during PE (4,5,19). Furthermore, PA clot load scores do not take into account clots located in small peripheral PAs; the Miller, Walsh, and Mastora scores consider segmental PAs and the Qanadli score con-

Teaching Point

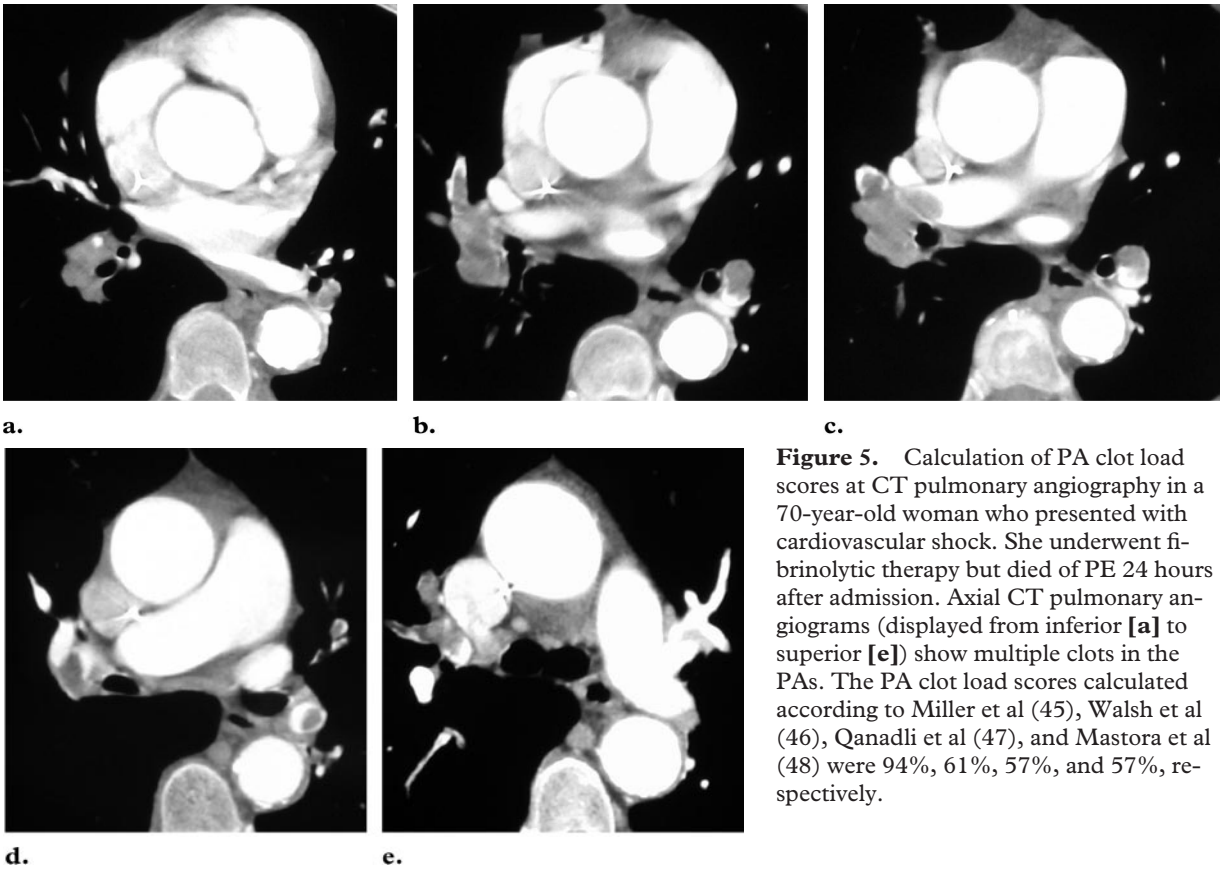

Figure 5. Calculation of PA clot load scores at CT pulmonary angiography in a 70-year-old woman who presented with cardiovascular shock. She underwent fibrinolytic therapy but died of PE 24 hours after admission. Axial CT pulmonary angiograms (displayed from inferior **[a]** to superior **[e]**) show multiple clots in the PAs. The PA clot load scores calculated according to Miller et al (45), Walsh et al (46), Qanadli et al (47), and Mastora et al (48) were 94%, 61%, 57%, and 57%, respectively.

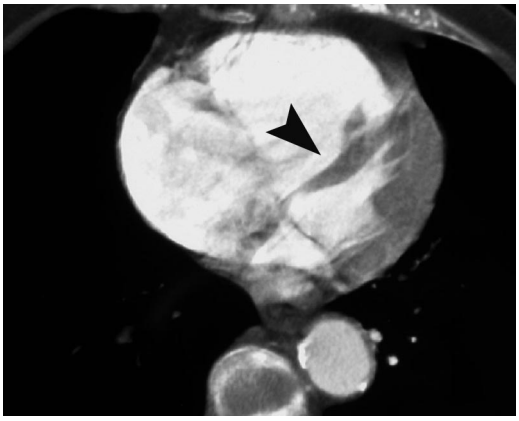

Figure 6. Acute dilatation of the RV with leftward septal bowing in a 68-year-old woman who presented with severe dyspnea and severe hypotension. CT pulmonary angiography showed massive PE, and the PA clot load score calculated according to Qanadli et al (47) was 57%. She underwent a Trendelenburg intervention but died during the first 24 hours after admission. Axial CT pulmonary angiogram obtained at the level of the heart shows signs of cor pulmonale. Note the severe dilatation of the RV and the compression of the LV: The short-axis diameters of the RV and LV were 59.4 mm and 24 mm, respectively, and the RV/LV diameter ratio was 2.5. Also note the leftward bowing of the interventricular septum (arrowhead).

siders subsegmental PAs the most distal arteries (45–49). Finally, PA clot load scores do not take into account possible unresolved previous episodes of PE, emphysema, or other restrictive pleuroparenchymal disease that may contribute to an increase in PA pressure (37).

PA Diameter Measurement

A PA diameter greater than 30 mm indicates a PA pressure greater than 20 mm Hg (51). Collomb et al (37) showed that the diameter of the main PA was significantly different between patients with severe PE and patients with nonsevere PE. The diameter of the main PA or the ratio of the diameters of the main PA and the aorta was not an indicator of mortality or severity of acute PE in three other studies (38,39,42). Qanadli et al (47) reported a poor correlation between the PA clot load scores and the mean PA pressure.

Leftward Bowing of the Interventricular Septum

Leftward bowing of the interventricular septum at CT has been related to severe PA obstruction (52) (Fig 6). Collomb et al (37) and Araoz et al

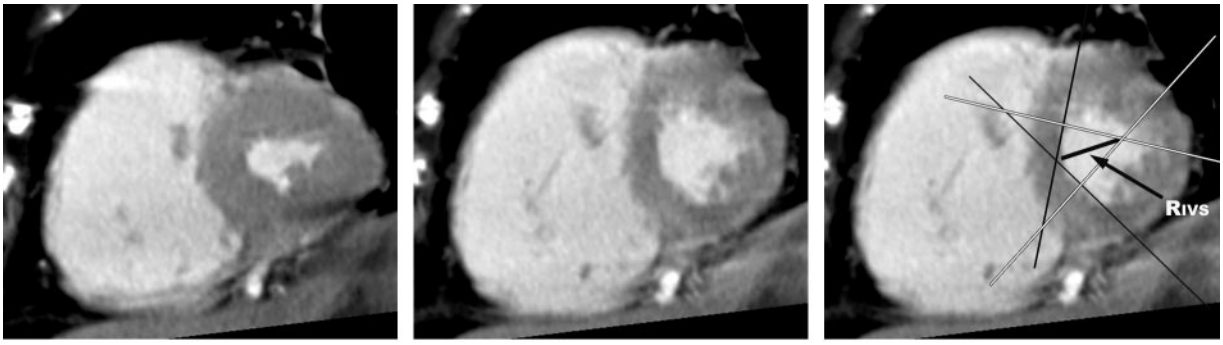

Figure 7. Severe dilatation of the RV with septal flattening in diastole in a 67-year-old woman with massive PE. The patient underwent fibrinolytic therapy immediately after diagnosis. **(a, b)** CT images of the short axes of the ventricles show that the RV is severely dilated relative to the LV. Unlike the LV, the RV demonstrates little variation in volume between systole **(a)** and diastole **(b)**. Note the flattening of the interventricular septum in diastole. **(c)** CT image shows quantification of the septal flattening. The thin black lines delineate the endocardial borders of the interventricular septum. The white lines are drawn perpendicular to the thin black lines at the mid distances of the endocardial borders. The radius of the interventricular septum (R_{IVS}) is measured from the intersection of the white lines to the endocardial border (53).

(42) found this sign to be an indicator of the severity of PE or of subsequent admission to the intensive care unit. However, this sign does not seem to be an indicator of outcome (38,39,42) and is not specific for PE, as it can be found in numerous causes of chronic PA hypertension (37). In chronic PA hypertension, the RV wall is usually thickened (>6 mm [normal value, approximately 4 mm]), a finding that is not seen in acute PE (21,30). Quantification of septal bowing by means of echocardiography can be applied to CT (Fig 7) (53).

Reflux of Contrast Medium into the IVC

Another upstream manifestation of acute right heart failure is the reflux of contrast medium into the IVC, which has recently been described as a predictor of mortality in patients with severe PE (39). Reflux of contrast medium into the IVC is an indirect sign of tricuspid valve insufficiency, frequently observed in right heart failure (35,54). During severe acute PE, tricuspid regurgitation may develop as a result of RV dilatation, further reducing RV output (35). Nevertheless, Collomb et al (37) did not find a significant difference between patients with severe PE and patients with nonsevere PE in regard to this sign.

Experimental Findings and Future Issues

Assessment of Pulmonary Perfusion

The limitation of the PA clot load score of being restricted to segmental or subsegmental PAs could be overcome by assessment of pulmonary perfusion at the level of the microcirculation. The extent of PE has previously been assessed by quantification of perfusion defects at ventilation-perfusion lung scanning, pulmonary angiography, and magnetic resonance (MR) imaging. Three- to 5-mm subsegmental emboli have been reported to create 3–5-cm perfusion defects in the peripheral parenchyma (55).

Oligemia, defined as a geographic area of decreased parenchymal CT attenuation associated with abnormally small pulmonary blood vessels, was found to be associated with a higher risk of subsequent intubation or subsequent use of vasopressors in the study by Araoz et al (42). However, this sign is not specific for PE and may be found in patients with airway disease (42).

New areas of research are dedicated to providing morphologic and functional information about the effect of PE on lung perfusion by using a single modality, similar to MR imaging. The pulmonary blood flow can thus be assessed noninvasively at a microvascular level, providing

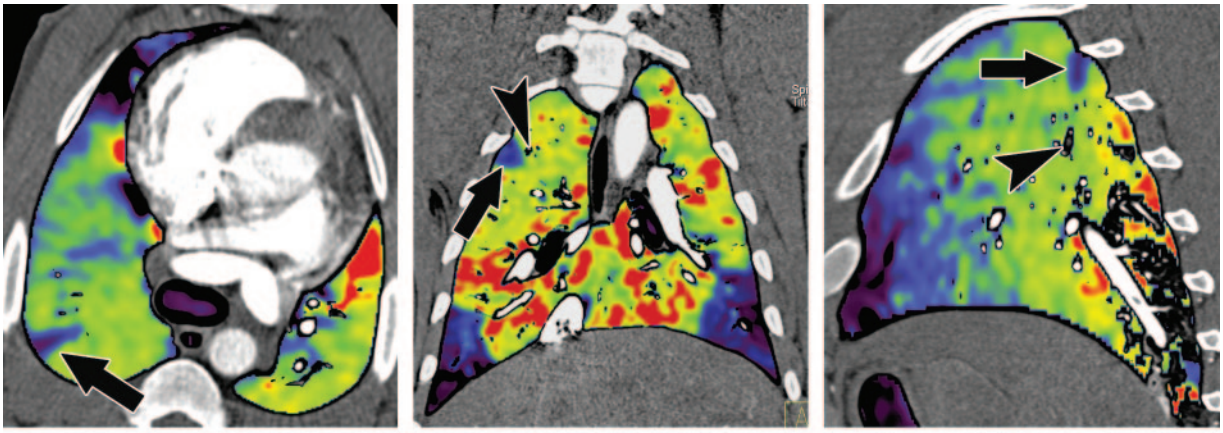

a. b. c.

Figure 8. Perfusion of the lung parenchyma assessed with subtraction color-coded CT after experimental clot embolization in the PAs of a pig. Axial **(a)**, coronal **(b)**, and sagittal **(c)** CT images show multiple subsegmental perfusion defects, which are displayed in blue (arrow). The triangular perfusion defects are suggestive of emboli in small peripheral PAs. On the coronal and sagittal images, note the additional occluding subsegmental emboli (arrowhead in **b** and **c**) with resulting small peripheral perfusion defects (arrow). (Courtesy of Joachim Wildberger, MD, University Hospital of Aachen, Germany.)

quantification of the percentage of lung parenchyma with impaired microcirculation. Dynamic pulmonary angiography acquisition with electron-beam CT, performed by using high-flow (10 mL/sec) contrast medium injection, allowed visualization of perfusion defects and generation of color-coded maps of peak attenuation change, time to peak enhancement, and mean transit time of contrast medium over a limited lung volume in patients with proved PE at a previous CT pulmonary angiography examination (56). Drawbacks were partially occluded vessels, a limited length of acquisition, and the need for repeat scanning and injection of contrast medium after diagnostic CT pulmonary angiography (55).

Wildberger et al (57) reported preliminary results of perfusion-weighted color maps directly obtained from CT pulmonary angiography acquisition after automated three-dimensional segmentation of the lungs, including suppression of vessels and major airways. Inhomogeneities due to underlying lung disease, such as emphysema or condensation, remain a drawback of this technique. Using 16-detector-row helical CT, Wildberger et al (55,58) applied a dual-phase subtraction technique, before and after injection of 80 mL of contrast medium at a flow rate of 4 mL/sec, to an animal model of PE (Fig 8). Drawbacks remain double radiation and the breath-hold time (around 30 seconds), as both nonenhanced and contrast-enhanced acquisitions have to be performed during a single apnea. The advent of faster CT scanning with an increased number of detector rows or x-ray tubes should result in the emergence of research on this topic.

Dynamic and Functional Cardiac Assessment

Teaching Point

The advent of multidetector CT and data acquisition coupled with ECG-gated recording is leading to the ability to perform dynamic and functional assessment of the RV.

Ejection Fraction.—A recent study by Coche et al (59) assessed the feasibility of performing cardiac function measurement with retrospective ECG-gated multidetector CT pulmonary angiography in patients suspected of having PE. Contiguous thin sections can be reconstructed every 5%–10% of the R-R interval, and the RV and LV ejection fraction can be calculated by using

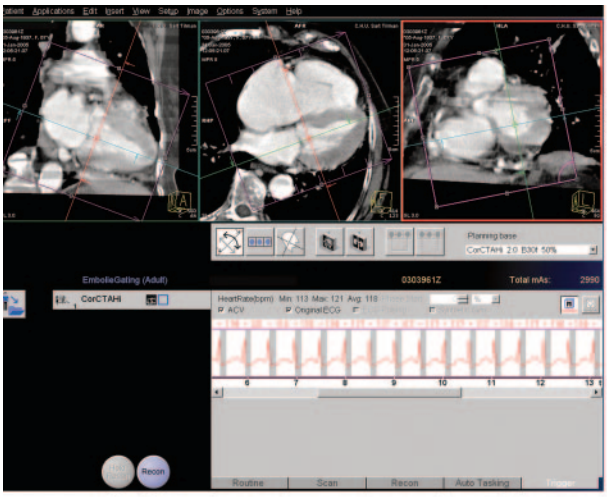

a.

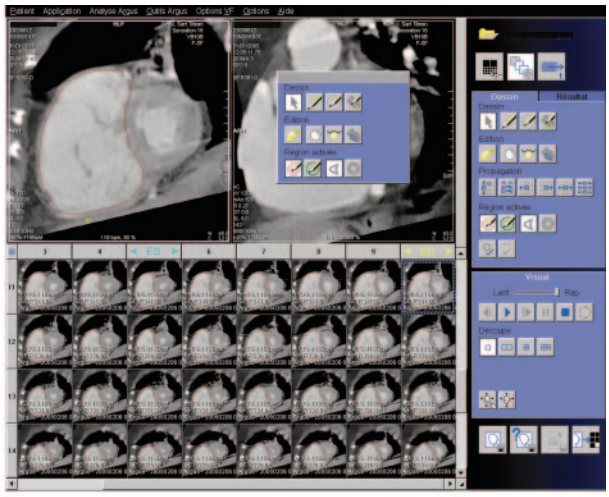

b.

Patient ID: 0303961Z	Examination Date: 31/01/2005			
Patient Height: 160.00 cm.	Patient Weight: 61.00 kg.		Heart Rate: 118 Beats/min	
Right Ventricle - Absolute				
Cardiac Function			Normal Range (F) (CT)	Units
Ejection Fraction	EF	17.2	47.00 ... 80.00	%
End Diastolic Volume	EDV	218.0	58.00 ... 154.00	ml
End Systolic Volume	ESV	180.5	12.00 ... 68.00	ml
Stroke Volume	SV	37.5	35.00 ... 98.00	ml
Cardiac Output	CO	4.43	2.65 ... 5.98	l/min
Myocardial Mass (at ED)		----	----	g
Myocardial Mass (Avg)		----	----	g
Filling and Ejection Data				
Peak Ejection Rate		698.8	n.a.	ml/sec
Peak Ejection Time		0.0	n.a.	msec
Peak Filling Rate		1562.6	n.a.	ml/sec
Peak Filling Time from ES		20.0	n.a.	msec

c.

Figure 9. Calculation of the RV ejection fraction with CT in a 67-year-old woman with massive PE (same patient as in Fig 7). **(a)** After ECG-gated CT pulmonary angiography, the box for short-axis reformation is applied inside the CT raw data volume (images at top of computer screen). Reformatted short-axis CT sections are usually 5–8 mm thick. Multiple series of reformatted images are obtained every 5%–10% of the R-R cycle. **(b)** Computer screen shows series of short-axis images of the heart, which were generated every 10% of the R-R cycle. Manual contouring was then performed along the inner wall of the RV for each series by using dedicated software (Argus; Siemens Medical Solutions, Erlangen, Germany). **(c)** List of the results provided by the software shows that the end-systolic and end-diastolic volumes are dramatically enlarged, whereas the ejection fraction is reduced to 17%.

dedicated three-dimensional software (Fig 9). Two recent studies have demonstrated that the results of such measurement of the RV ejection fraction are comparable with those of the scintigraphic technique and are reproducible (59,60). Work in progress is currently assessing if measurement of the RV ejection fraction with CT pulmonary angiography can provide further refinements in prediction of the outcome in patients with PE.

RV Wall Motion Abnormality.—It has been demonstrated at echocardiography that a regional RV wall motion abnormality in which the apex is spared (McConnell sign) is a PE-specific pattern of RV dysfunction (29). No study has currently assessed if RV wall motion abnormalities could be identified at CT pulmonary angiography performed with ECG-gated acquisition and if this finding could be used as a more powerful predictor of outcome related to acute PE than is the RV/LV diameter ratio.

Patency of the Foramen Ovale

A relationship between the frequency of foramen ovale patency, responsible for right-to-left shunting, and the severity of PE vascular obstruction at scintigraphy has been demonstrated (61). The echocardiographic detection of a patent foramen ovale has also been shown to be associated with a significantly increased complicated clinical course (including paradoxical embolism). An overall mortality of 33% was reported in patients with major PE and a patent foramen ovale versus an overall mortality of 14% in those without a patent foramen ovale (62). Unlike the detection of large atrial septal defects, the detection of foramen ovale patency with ECG-gated multidetector CT currently remains difficult (63,64). Nevertheless, it remains to be demonstrated whether the increased temporal and spatial resolution of a new generation of multidetector CT scanners will allow recognition of foramen ovale patency. The presence of a saddle clot within the foramen ovale should facilitate the diagnosis (Fig 10; see also Movie 1 at *radiographics.rsnajnls.org/cgi/content/full/26/1/23/DC1*).

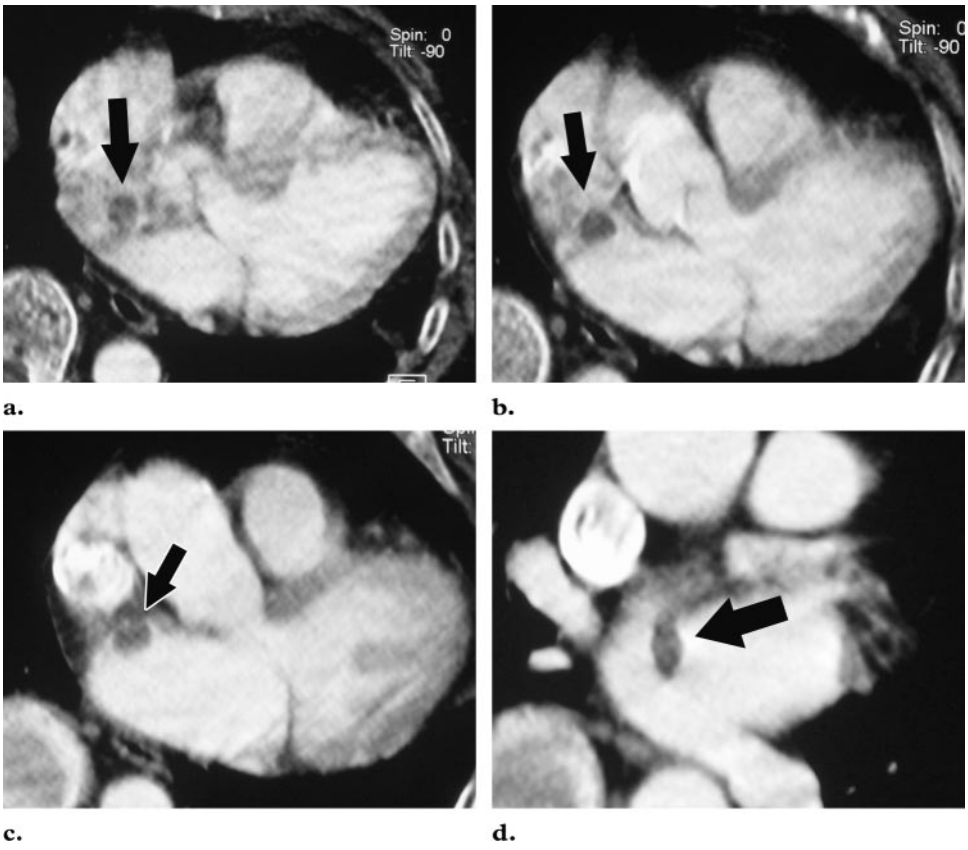

Figure 10. Saddle clot passing through a patent foramen ovale in a 70-year-old woman who presented with PA hypertension secondary to massive acute PE. Axial CT pulmonary angiograms show a saddle clot (arrow) passing from the right atrium **(a)** through a patent foramen ovale **(b)** into the left atrium **(c, d)**.

Clot Burden at the Level of Lower Limb and Abdominal Veins

Although clots in the PAs influence the cardiopulmonary status of the patients, the major risk of death is from recurrent PE, which in more than 90% of the patients originates from lower limb veins (2,7,8,65). Therefore, investigation of lower limb veins has been part of diagnostic algorithms in patients suspected of having PE. Imaging and estimation of the volume of the clot burden in lower limb veins may therefore be another important CT finding to consider for management, treatment, and prognosis in patients with PE.

Various scoring systems for venous thrombosis are reported in the literature (66–72). In 1977, Marder et al (66) developed a venographic score to evaluate streptokinase and heparin therapy. The Marder score is still the most commonly used in anticoagulant drug trials, although its validity has never been proved. The Arnesen score and the Mewissen score (or American Venous Registry index) were designed to assess the response of venous thrombosis to anticoagulant or fibrinolytic therapy (67,68). The Porter score or SVS/ISCVS (Society for Vascular Surgery/International Society for Cardiovascular Surgery) index, originally described in 1988 and refined in 1995, was developed in an attempt to standardize the reporting criteria for venous thromboembolic disease and was designed to be applicable for both venography and US (69,70).

The previous scores were not validated and, because they do not consider all the different lower limb veins, underestimate the thrombotic burden of deep venous thrombosis (DVT). The Ouriel score, reported in 1999, was designed to provide a more accurate quantitative estimate of the thrombus mass by calculating a volumetric index for all the venous segments (71). The Björgell score, described in 1999, was designed to be applicable to venography, US, CT, and MR imaging (72). Details on calculation of venous clot load scores are presented in Appendix 2.

Speculative interpretations such as "smaller venous clots produce less severe PE" or "the probability of finding residual DVT is higher in patients with more severe PE" have been reported (73). To our knowledge, only two studies have

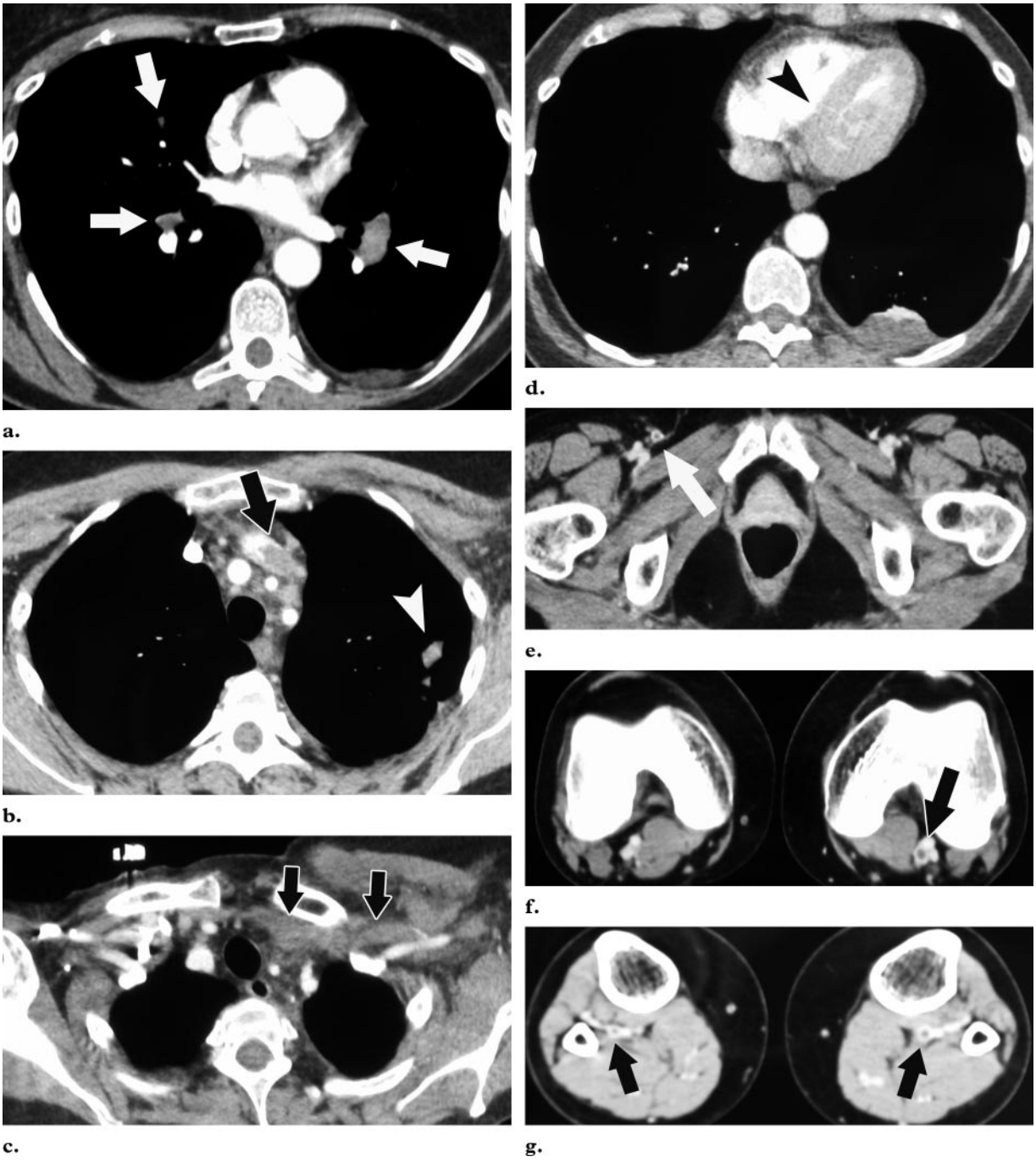

Figure 11. Massive PE, dilatation of the right side of the heart with septal flattening, incidentally discovered lung cancer, and multiple paraneoplastic venous thromboses in a 61-year-old woman who presented with increasing dyspnea and alteration of her general condition. The pathologic conditions were diagnosed with combined CT pulmonary angiography–CT venography. **(a–d)** Axial CT pulmonary angiograms obtained with a 16-detector-row scanner show the following findings: multiple PEs in the segmental PAs of both lower lobes and the middle lobe (arrows in **a**); a lung carcinoma in the left upper lobe (arrowhead in **b**); thrombi in the left innominate and left subclavian veins (arrow in **b**, arrows in **c**); and an RV that is dilated relative to the LV with associated flattening of the interventricular septum (arrowhead in **d**). **(e–g)** Axial CT venograms show multiple venous clots in the right great saphenous vein (arrow in **e**), left popliteal vein (arrow in **f**), and bilateral tibioperoneal trunks (arrows in **g**).

assessed the different DVT severity scores in patients with PE. Although their methodology and the small numbers of patients precluded statistical analysis, Ouriel et al (71) reported a higher mean DVT severity score in patients with proved PE than in patients with DVT but without clinically significant PE. They also reported that PE can be observed in patients with a low DVT severity score.

Another study by Ghaye et al (74) showed a good correlation of all the previously described DVT severity scoring systems with each other. On the other hand, PE and DVT severity scores correlated only poorly to moderately, particularly in patients without symptoms of DVT, indicating that the severity of both aspects of venous thromboembolism cannot be predicted from the assessment of one aspect only. In a large percentage of patients, a low PE score is associated with a low DVT score. In some patients, DVT limited to the calf (low score) can be associated with massive PE (high score). Conversely, patients with peripheral PE (low score) may have clots located in the iliofemoral veins (high score) (74).

In the PIOPED (Prospective Investigation of Pulmonary Embolism Diagnosis) study, 90% of the patients who died of PE actually died of recurrent PE (75). It would therefore be useful to investigate if the rate of recurrent PE is higher in patients with a high DVT score. Such findings may have implications for patient care (strict bed rest, elastic stockings, IVC filter, etc) and emphasize the importance of a global work-up of the venous thromboembolic disease. Therefore, combined CT pulmonary angiography–CT venography is particularly well-suited for calculation of DVT and PE severity scores and cardiovascular CT findings in a single examination (Fig 11; see also Movie 2 at *radiographics.rsnajnls.org/cgi/content/full/26/1/23/DC1*).

Conclusions

Teaching Point

PE associated with RV failure is frequently lethal. Risk stratification of patients with PE is important because optimal management, monitoring, and therapeutic strategies depend on the prognosis. Recent studies have demonstrated that CT pulmonary angiography not only allows diagnosis of PE but also enables accurate assessment of PE severity in a single examination. Cardiovascular CT findings, such as the RV/LV diameter ratio, have shown a significant correlation with fatal outcome, whereas quantification of PA clot load remains controversial. Many CT findings that may allow refinement of the risk stratification are still under evaluation.

Appendix 1: PA Clot Load Scores

Miller Score

The right PA has nine major segmental branches (three to the upper lobe, two to the middle lobe, and four to the lower lobe). The left PA has seven major branches (two to the upper lobe, two to the lingula, and three to the lower lobe). The presence of a filling defect or obstruction in any one of these branches scores 1 point. A filling defect proximal to segmental branches scores a value equal to the number of segmental branches arising distally. The maximum score is 9 for the right lung and 7 for the left lung. The maximum possible CT obstruction score is 16 for both lungs. In addition, the score originally evaluated the effect of embolism on PA flow, which currently cannot be assessed with CT pulmonary angiography (45).

Walsh Score

The maximum score is 18 for both lungs. Different scores are given for filling defects and obstructions and for anatomic locations. The following guidelines govern quantification of embolic abnormalities: *(a)* Abnormalities in a single segmental PA receive a total score that does not exceed 1, regardless of the type or number of abnormalities. *(b)* The total maximum score is 3 for abnormalities in a single upper lobar region, 2 for abnormalities in the middle lobe or lingula, and 4 for abnormalities in the lower lobes. *(c)* Obstructions in central anatomic regions receive scores according to the vessel involved. *(d)* If the total score for one lung is greater than 4 without considering filling defects in central regions, the central filling defects are ignored. All filling defects in a single central region, whether single or multiple, receive a score of 3. *(e)* If a single vessel contains both a filling defect and an obstruction, only the obstruction is scored. *(f)* The sum of scores for all abnormalities in one lung may not exceed a value of 9. The maximum CT obstruction score is 18 (46).

Qanadli Score

The arterial tree of each lung is regarded as having 10 segmental PAs (three to the upper lobes, two to the middle lobe or lingula, and five to the lower lobes). The presence of an embolus in a segmental PA is scored as 1 point, and emboli at the most proximal arterial level are scored a value equal to the number of segmental PAs arising distally. To provide additional information on the residual perfusion distal to the embolus, a weighting factor is used for each value (0 = no defect, 1 = partial occlusion, and 2 = complete occlusion). An isolated subsegmental embolus is considered a partially occluded segmental PA and is assigned a value of 1. The maximum CT obstruction index is 40 (47).

Mastora Score

The scoring is applied to five mediastinal PAs (PA trunk, right and left PAs, and right and left interlobar PAs); six lobar PAs; and 20 segmental PAs (three in the upper lobes, two in the middle lobe or lingula, and five in the lower lobes). The CT severity score is based on the percentage of obstructed surface of each central and peripheral PA section and uses a 5-point scale (1 = <25%, 2 = 25%–49%, 3 = 50%–74%, 4 = 75%–99%, 5 = 100%). A central score (mediastinal and lobar PAs), a peripheral score (segmental PAs), and a global score (central and peripheral PAs) can be calculated. The maximum CT obstruction score is 155 (48).

For comparison between each other, all scores can be expressed as a percentage of vascular obstruction and calculated by dividing the patient's score by the maximum total score and multiplying the results by 100 (range, 0%–100%).

Appendix 2: Clot Load Scores from Lower Limb Veins

Marder Score

Eight venous segments are concerned. The maximum score allowed each segment varies from 2 to 10 points, reflecting the calculated volume of each segment. Included segments are the common iliac veins, external iliac veins, common femoral veins, superficial femoral veins, popliteal veins, anterior tibial veins, posterior tibial veins, and peroneal veins. A maximum score of 40 points per limb can be obtained. Total exclusion or nonfilling of a vein is assigned the maximum score per segment, whereas partial exclusion or filling defects are assigned a lower score in proportion to the degree of involvement (66).

American Venous Registry or Mewissen Score

Seven venous segments are included: the IVC, common iliac veins, external iliac veins, common femoral veins, proximal superficial femoral veins, distal superficial femoral veins, and popliteal veins. The score is based on partial or complete occlusion of each segment (0–2). The maximum score is 14 per limb (67).

Arnesen Score

Six deep vein segments are included: the iliac veins, femoral veins, popliteal veins, anterior tibial veins, posterior tibial veins, and peroneal veins. The score is based on the relative volume of partial occlusion or the nonvisualization, due to complete occlusion, of each segment (0–5). The maximum score is 30 per limb (68).

Porter Score

Six deep veins and two superficial vein segments are included. Included segments are the IVC, iliac veins, common or superficial femoral veins, deep femoral veins, popliteal veins, tibial or soleal veins, and greater and lesser saphenous veins. The score is based on the subsegmental or segmental and nonocclusive or occlusive aspect of each segment (0–3). The maximum score is 24 per limb (69,70).

Ouriel Score

Fourteen venous segments are considered. Included segments are the IVC, common iliac veins, external iliac veins, internal iliac veins, common femoral veins, superficial femoral veins, deep femoral veins, and popliteal veins and segments of the anterior tibial veins, posterior tibial veins, and peroneal veins. A normalized volumetric score is calculated for each segment by combining measurements from CT, US, and venography. Partially occluded veins are assigned a score of one-half the score value for the segment. The score varies from 1 for a single calf vein to 26 for the IVC. The maximum score is 63 per limb (71).

Bjorgell Score

This score was described in 1999 and was designed to be applicable to venography, US, CT, and MR imaging. Twelve different vein segments are considered: the IVC, common iliac veins, external iliac veins, common femoral veins, superficial femoral veins, deep femoral veins, popliteal veins, gastrocnemius veins, anterior tibial veins, posterior tibial veins, peroneal veins, and sural veins. The score is based on the relative length of the thrombus in each segment (0–3). The maximum score is 36 per limb (72).

References

1. Cushman M, Tsai AW, White RH, et al. Deep vein thrombosis and pulmonary embolism in two cohorts: the longitudinal investigation of thromboembolism etiology. Am J Med 2004;117:19–25.
2. Goldhaber SZ, Visani L, De Rosa M. Acute pulmonary embolism: clinical outcomes in the International Cooperative Pulmonary Embolism Registry (ICOPER). Lancet 1999;353:1386–1389.
3. Kasper W, Konstantinides S, Geibel A, et al. Management strategies and determinants of outcome in acute major pulmonary embolism: results of a multicenter registry. J Am Coll Cardiol 1997;30:1165–1171.
4. Wood KE. Major pulmonary embolism: review of a pathophysiologic approach to the golden hour of hemodynamically significant pulmonary embolism. Chest 2002;121:877–905.
5. Lualdi JC, Goldhaber SZ. Right ventricular dysfunction after acute pulmonary embolism: pathophysiologic factors, detection, and therapeutic implications. Am Heart J 1995;130:1276–1282.

6. Ribeiro A, Lindmarker P, Juhlin-Dannfelt A, Johnsson H, Jorfeldt L. Echocardiography Doppler in pulmonary embolism: right ventricular dysfunction as a predictor of mortality rate. Am Heart J 1997;134:479–487.
7. Kasper W, Konstantinides S, Geibel A, Tiede N, Krause T, Just H. Prognostic significance of right ventricular afterload stress detected by echocardiography in patients with clinically suspected pulmonary embolism. Heart 1997;77:346–349.
8. Grifoni S, Olivotto I, Cecchini P, et al. Short-term clinical outcome of patients with acute pulmonary embolism, normal blood pressure, and echocardiographic right ventricular dysfunction. Circulation 2000;101:2817–2822.
9. Konstantinides S, Geibel A, Heusel G, et al. Heparin plus alteplase compared with heparin alone in patients with submassive pulmonary embolism. N Engl J Med 2002;347:1143–1150.
10. Konstantinides S, Geibel A, Olschewski M, et al. Association between thrombolytic treatment and the prognosis of hemodynamically stable patients with major pulmonary embolism: results of a multicenter registry. Circulation 1997;96:882–888.
11. Goldhaber SZ. Echocardiography in the management of pulmonary embolism. Ann Intern Med 2002;136:691–700.
12. Ghaye B, Remy J, Remy-Jardin M. Non-traumatic thoracic emergencies: CT diagnosis of acute pulmonary embolism—the first 10 years. Eur Radiol 2002;12:1886–1905.
13. Schoepf UJ, Costello P. CT angiography for diagnosis of pulmonary embolism: state of the art. Radiology 2004;230:329–337.
14. Musset D, Parent F, Meyer G, et al. Diagnostic strategy for patients with suspected pulmonary embolism: a prospective multicentre outcome study. Lancet 2002;360:1914–1920.
15. Fedullo PF, Tapson VF. The evaluation of suspected pulmonary embolism. N Engl J Med 2003; 349:1247–1256.
16. Perrier A, Nendaz MR, Sarasin FP, Howarth N, Bounameaux H. Cost-effectiveness analysis of diagnostic strategies for suspected pulmonary embolism including helical computed tomography. Am J Respir Crit Care Med 2003;167:39–44.
17. Gurney JW. No fooling around: direct visualization of pulmonary embolism [editorial]. Radiology 1993;188:618–619.
18. Quiroz R, Kucher N, Schoepf UJ, et al. Right ventricular enlargement on chest computed tomography: prognostic role in acute pulmonary embolism. Circulation 2004;109:2401–2404.
19. Smulders YM. Pathophysiology and treatment of haemodynamic instability in acute pulmonary embolism: the pivotal role of pulmonary vasoconstriction. Cardiovasc Res 2000;48:23–33.
20. Ghuysen A, Lambermont B, Dogne JM, et al. Effect of BM-573 [N-terbutyl-N′-[2-(4′-methylphenylamino)-5-nitro-benzenesulfonyl]urea], a dual thromboxane synthase inhibitor and thromboxane receptor antagonist, in a porcine model of acute pulmonary embolism. J Pharmacol Exp Ther 2004;310:964–972.
21. Jardin F, Dubourg O, Bourdarias JP. Echocardiographic pattern of acute cor pulmonale. Chest 1997;111:209–217.
22. Belenkie I, Dani R, Smith ER, Tyberg JV. The importance of pericardial constraint in experimental pulmonary embolism and volume loading. Am Heart J 1992;123:733–742.
23. Contractor S, Maldjian PD, Sharma VK, Gor DM. Role of helical CT in detecting right ventricular dysfunction secondary to acute pulmonary embolism. J Comput Assist Tomogr 2002;26:587–591.
24. Kucher N, Walpoth N, Wustmann K, Noveanu M, Gertsch M. QR in V1: an ECG sign associated with right ventricular strain and adverse clinical outcome in pulmonary embolism. Eur Heart J 2003;24:1113–1119.
25. Kucher N, Goldhaber SZ. Cardiac biomarkers for risk stratification of patients with acute pulmonary embolism. Circulation 2003;108:2191–2194.
26. Moreno FL, Hagan AD, Holmen JR, Pryor TA, Strickland RD, Castle CH. Evaluation of size and dynamics of the inferior vena cava as an index of right-sided cardiac function. Am J Cardiol 1984; 53:579–585.
27. Kircher BJ, Himelman RB, Schiller NB. Noninvasive estimation of right atrial pressure from the inspiratory collapse of the inferior vena cava. Am J Cardiol 1990;66:493–496.
28. Mansencal N, Joseph T, Vieillard-Baron A, et al. Comparison of different echocardiographic indexes secondary to right ventricular obstruction in acute pulmonary embolism. Am J Cardiol 2003; 92:116–119.
29. McConnell MV, Solomon SD, Rayan ME, Come PC, Goldhaber SZ, Lee RT. Regional right ventricular dysfunction detected by echocardiography in acute pulmonary embolism. Am J Cardiol 1996; 78:469–473.
30. Prakash R, Matsukubo H. Usefulness of echocardiographic right ventricular measurements in estimating right ventricular hypertrophy and right ventricular systolic pressure. Am J Cardiol 1983; 51:1036–1040.
31. Vieillard-Baron A, Qanadli SD, Antakly Y, et al. Transesophageal echocardiography for the diagnosis of pulmonary embolism with acute cor pulmonale: a comparison with radiological procedures. Intensive Care Med 1998;24:429–433.
32. McIntyre KM, Sasahara AA. Correlation of pulmonary photoscan and angiogram as measures of the severity of pulmonary embolic involvement. J Nucl Med 1971;12:732–738.
33. McDonald IG, Hirsh J, Hale GS, O'Sullivan EF. Major pulmonary embolism: a correlation of clinical findings, haemodynamics, pulmonary angiography, and pathological physiology. Br Heart J 1972;34:356–364.
34. Alpert JS, Smith R, Carlson J, Ockene IS, Dexter L, Dalen JE. Mortality in patients treated for pulmonary embolism. JAMA 1976;236:1477–1480.
35. Miller RL, Das S, Anandarangam T. Association between right ventricular function and perfusion abnormalities in hemodynamically stable patients with acute pulmonary embolism. Chest 1998;113: 665–670.
36. Reid JH, Murchison JT. Acute right ventricular dilatation: a new helical CT sign of massive pulmonary embolism. Clin Radiol 1998;53:694–698.
37. Collomb D, Paramelle PJ, Calaque O, et al. Severity assessment of acute pulmonary embolism: evaluation using helical CT. Eur Radiol 2003;13: 1508–1514.

38. van der Meer RW, Pattynama PM, van Strijen MJ, et al. Right ventricular dysfunction and pulmonary obstruction index at helical CT: prediction of clinical outcome during 3-month follow-up in patients with acute pulmonary embolism. Radiology 2005;235:798–803.
39. Ghaye B, Ghuysen A, Willems V, et al. Pulmonary embolism CT severity scores and CT cardiovascular parameters as predictor of mortality in patients with severe pulmonary embolism. Radiology (in press).
40. Lim KE, Chan CY, Chu PH, Hsu YY, Hsu WC. Right ventricular dysfunction secondary to acute massive pulmonary embolism detected by helical computed tomography pulmonary angiography. Clin Imaging 2005;29:16–21.
41. Wintersperger BJ, Stabler A, Seemann M, et al. Evaluation of right heart load with spiral CT in patients with acute lung embolism [in German]. Rofo 1999;170:542–549.
42. Araoz PA, Gotway MB, Trowbridge RL, et al. Helical CT pulmonary angiography predictors of in-hospital morbidity and mortality in patients with acute pulmonary embolism. J Thorac Imaging 2003;18:207–216.
43. Schoepf UJ, Kucher N, Kipfmueller F, Quiroz R, Costello P, Goldhaber SZ. Right ventricular enlargement on chest computed tomography: a predictor of early death in acute pulmonary embolism. Circulation 2004;110:3276–3280.
44. Milne ENC, Pistolesi M. Assessing systemic intra- and extravascular water. In: Milne ENC, Pistolesi M, eds. Reading the chest radiograph: a physiologic approach. St Louis, Mo: Mosby, 1993; 80–119.
45. Miller GA, Sutton GC, Kerr IH, Gibson RV, Honey M. Comparison of streptokinase and heparin in treatment of isolated acute massive pulmonary embolism. Br Med J 1971;2:681–684.
46. Walsh PN, Greenspan RH, Simon M, et al. An angiographic severity index for pulmonary embolism. Circulation 1973;47-48(suppl):101–108.
47. Qanadli SD, El Hajjam M, Vieillard-Baron A, et al. New CT index to quantify arterial obstruction in pulmonary embolism: comparison with angiographic index and echocardiography. AJR Am J Roentgenol 2001;176:1415–1420.
48. Mastora I, Remy-Jardin M, Masson P, et al. Severity of acute pulmonary embolism: evaluation of a new spiral CT angiographic score in correlation with echocardiographic data. Eur Radiol 2003;13:29–35.
49. Bankier AA, Janata K, Fleischmann D, et al. Severity assessment of acute pulmonary embolism with spiral CT: evaluation of two modified angiographic scores and comparison with clinical data. J Thorac Imaging 1997;12:150–158.
50. Wu AS, Pezzullo JA, Cronan JJ, Hou DD, Mayo-Smith WW. CT pulmonary angiography: quantification of pulmonary embolus as a predictor of patient outcome—initial experience. Radiology 2004;230:831–835.
51. Kuriyama K, Gamsu G, Stern RG, Cann CE, Herfkens RJ, Brundage BH. CT-determined pulmonary artery diameters in predicting pulmonary hypertension. Invest Radiol 1984;19:16–22.
52. Oliver TB, Reid JH, Murchison JT. Interventricular septal shift due to massive pulmonary embolism shown by CT pulmonary angiography: an old sign revisited. Thorax 1998;53:1092–1094.
53. Klima UP, Lee MY, Guerrero JL, Laraia PJ, Levine RA, Vlahakes GJ. Determinants of maximal right ventricular function: role of septal shift. J Thorac Cardiovasc Surg 2002;123:72–80.
54. Kurzman P, Yeh BM, Foster E, Qayyum A, Coakley FV. Determinants of retrograde inferior vena cava or hepatic vein opacification during contrast-enhanced CT (abstr). In: Radiological Society of North America scientific assembly and annual meeting program. Oak Brook, Ill: Radiological Society of North America, 2003; 412.
55. Wildberger JE, Schoepf UJ, Mahnken AH, et al. Approaches to CT perfusion imaging in pulmonary embolism. Semin Roentgenol 2005;40:64–73.
56. Schoepf UJ, Bruening R, Konschitzky H, et al. Pulmonary embolism: comprehensive diagnosis by using electron-beam CT for detection of emboli and assessment of pulmonary blood flow. Radiology 2000;217:693–700.
57. Wildberger JE, Niethammer MU, Klotz E, Schaller S, Wein BB, Gunther RW. Multi-slice CT for visualization of pulmonary embolism using perfusion weighted color maps. Rofo 2001;173:289–294.
58. Wildberger JE, Klotz E, Ditt H, Spuntrup E, Mahnken AH, Gunther RW. Multislice computed tomography perfusion imaging for visualization of acute pulmonary embolism: animal experience. Eur Radiol 2005;15:1378–1386.
59. Coche E, Vlassenbroek A, Roelants V, et al. Evaluation of biventricular ejection fraction with ECG-gated 16-slice CT: preliminary findings in acute pulmonary embolism in comparison with radionuclide ventriculography. Eur Radiol 2005;15:1432–1440.
60. Delhaye D, Teisseire A, Bruzzi J, et al. Les fractions d'éjection en angioscanographie multicoupe du thorax: comparaison avec la ventriculoscintigraphie isotopique à l'équilibre [abstract]. J Radiol 2004;85:1388.
61. Miller RL, Das S, Anandarangam T, et al. Relation between patent foramen ovale and perfusion abnormalities in acute pulmonary embolism. Am J Cardiol 1997;80:377–378.
62. Konstantinides S, Geibel A, Kasper W, Olschewski M, Blumel L, Just H. Patent foramen ovale is an important predictor of adverse outcome in patients with major pulmonary embolism. Circulation 1998;97:1946–1951.
63. Otsuka M, Itoh A, Haze K. Sinus venosus type of atrial septal defect with partial anomalous pulmonary venous return evaluated by multislice CT. Heart 2004;90:901.
64. Morgan-Hughes G, Marshall A, Roobottom C. Multi-detector row CT for the assessment of atrial septal defect and pulmonary venous drainage in adults [abstract]. Eur Radiol 2004;14(suppl 2):398.
65. Dalen JE, Alpert JS. Natural history of pulmonary embolism. Prog Cardiovasc Dis 1975;17:259–270.
66. Marder VJ, Soulen RL, Atichartakarn V, et al. Quantitative venographic assessment of deep vein thrombosis in the evaluation of streptokinase and heparin therapy. J Lab Clin Med 1977;89:1018–1029.

67. Mewissen MW, Seabrook GR, Meissner MH, Cynamon J, Labropoulos N, Haughton SH. Catheter-directed thrombolysis for lower extremity deep venous thrombosis: report of a national multicenter registry. Radiology 1999;211:39–49.
68. Arnesen H, Heilo A, Jakobsen E, Ly B, Skaga E. A prospective study of streptokinase and heparin in the treatment of deep vein thrombosis. Acta Med Scand 1978;203:457–463.
69. Porter JM, Moneta GL. Reporting standards in venous disease: an update. International Consensus Committee on Chronic Venous Disease. J Vasc Surg 1995;21:635–645.
70. Reporting standards in venous disease. Prepared by the Subcommittee on Reporting Standards in Venous Disease, Ad Hoc Committee on Reporting Standards, Society for Vascular Surgery/North American Chapter, International Society for Cardiovascular Surgery. J Vasc Surg 1988;8:172–181.
71. Ouriel K, Greenberg RK, Green RM, Massullo JM, Goines DR. A volumetric index for the quantification of deep venous thrombosis. J Vasc Surg 1999;30:1060–1066.
72. Bjorgell O, Nilsson PE, Svensson PJ, Bergqvist D. A new scoring system for the detailed description of the distribution and thrombotic burden in deep leg vein thrombosis. Angiology 1999;50:179–187.
73. Girard P, Musset D, Parent F, Maitre S, Phlippoteau C, Simonneau G. High prevalence of detectable deep venous thrombosis in patients with acute pulmonary embolism. Chest 1999;116:903–908.
74. Ghaye B, Willems V, Nchimi A, et al. Can quantification of clot load in the lower limb veins predict severity of pulmonary embolism in patients with venous thromboembolism? [abstract]. Eur Radiol 2004;14:237.
75. The PIOPED Investigators. Value of the ventilation/perfusion scan in acute pulmonary embolism: results of the Prospective Investigation of Pulmonary Embolism Diagnosis (PIOPED). JAMA 1990;263:2753–2759.

Teaching Points for Can CT Pulmonary Angiography Allow Assessment of Severity and Prognosis in Patients Presenting with Pulmonary Embolism?

Benoît Ghaye, MD, et al

RadioGraphics 2006; 26:23–40 • **Published online** 10.1148/rg.261055062 • **Content Codes:** CH CT

Page 24
The clinical impact of the embolic event depends not only on the embolus sizxe but also on the underlying cardiopulmonary status

Page 27
Additional studies have estimated that an RV/LV diameter ratio superior to 1.5 indicates a severe episode of PE (36–39, 41).

Page 28
Pulmonary vascular resistance is not only related to mechanical obstruction by the intravascular clot load but can be further increased by the release of vasoactive agents from plasma, platelets, or tissue; reflex PA vasoconstriction; and systemic arterial hypoxemia occurring during PE (4,5,19).

Page 31
The advent of multidetector CT and data acquisition coupled with ECG-gated recording is leading to the ability to perform dynamic and functional assessment of the RV.

Page 35
Risk stratification of patients with PE is important because optimal management, monitoring, and therapeutic strategies depend on the prognosis.